Exploration of the sum of flexoelectric coefficients of nematic liquid crystals

Hongyu Xing (邢红玉)[1,2,3], Wenjiang Ye (叶文江)[3], Naifu Wu (武乃福)[3], Zhidong Zhang (张志东)[3*], and Li Xuan (宣 丽)[1]

[1]*State Key Laboratory of Applied Optics, Changchun Institute of Optics, Fine Mechanics and Physics, Chinese Academy of Sciences, Changchun 130033, China*

[2]*Graduate University of Chinese Academy of Sciences, Beijing 100049, China*

[3]*School of Sciences, Hebei University of Technology, Tianjin 300401, China*

[*]*Corresponding author: zhidong_zhang@eyou.com*

Received September 26, 2011; accepted November 30, 2011; posted online January 17, 2012

We present a theoretical calculation of the dependence of reflectivity $R_{\rm pp}$ of the improved fully leaky waveguide geometry, which comprises pyramid, matching fluid, and strongly anchored hybrid−aligned nematic liquid crystal (NLC) cell on the internal angle. The calculation is based on the multi−layer optical theory and the elastic theory of liquid crystals. For different sums of flexoelectric coefficients e_{11} and e_{33}, the curve of $R_{\rm pp}$ moves a distance to the left or the right relative to the case of ignoring the flexoelectric effect and the distance of the movement varies with different flexoelectric coefficients. Consequently, the sum of flexoelectric coefficients can be explored by measuring the distance of the movement.

OCIS codes: 230.3720, 230.7390.
doi: 10.3788/COL201210.052301.

Liquid crystal displays (LCDs) are known as passive displays that depend on the nematic liquid crystal (NLC) filled in two pretreated substrates to modulate the incident linear polarized light when an external voltage is applied[1]. The orientation of deformation of the NLC has an important effect on display characteristics[2]. Some factors affecting the orientation of deformation of the NLC include the electric field, the anchoring of the substrate, and the flexoelectricity, among others. When two substrates are strongly anchored, the influence of the flexoelectric effect[3], induced by the splay or the bend deformation for the pear−shaped or banana−shaped NLC molecules with permanent dipoles, is predominant. The flexoelectric effect also bears on the electro−optical characteristics[4], threshold voltage[5], viewing angle characteristics[6], and electroconvection domain in a parallel−rubbed alignment cell[7], among others. All of these effects have a direct relationship with the flexoelectric coefficient.

The flexoelectric effect in liquid crystal was firstly proposed by Meyer in analyzing the piezoelectric effect in ordinary crystals in 1969[3]. Flexoelectric coefficients are generally acknowledged as in the order of 10^{-11} C/m[8], although the giant flexoelectric effect has been proposed by Harden *et al.*[9,10] as being in bent–core NLCs and bent–core NLC elastomers, in which the flexoelectric coefficient is larger by about 3–4 orders of magnitude than the conventional value. As a result, the flexoelectric effect can be easily covered by other effects, such as the dielectric effect, anchoring property, and adsorptive ions. Removing the influences of the above factors, some researchers have suggested different methods to measure the flexoelectric coefficient on the basis of the flexoelectric–optic effect[11−17]. In these methods, the optical guided wave method is more precise because the incident light and the transmitted and reflected light are selected as different polarized states, namely, p– or s–polarized state. Mazzulla *et al.*[15] studied the influence of both the flexoelectric effect and the surface polarization on a hybrid aligned nematic (HAN) cell using the half–leaky guided mode technique[18], and the sum of flexoelectric coefficients was determined at an external static field. However, this technique requires two high–refractive index substrates in the liquid crystal cell, which is not in agreement with the conventional liquid crystal device[19]. The improved fully leaky guided mode technique[20] can deal with the problem, and can be used to explore the sum of the flexoelectric coefficients e_{11} and e_{33} of NLCs. In this letter, we give a detailed theoretical analysis on this technique.

The geometry of the improved fully leaky liquid crystal waveguide is shown in Fig. 1. The lower substrate of the HAN cell is treated to induce a parallel anchoring of the director, whereas its upper substrate is treated to give a perpendicular anchoring. The HAN cell is inserted between two equilateral glass pyramids with optical contacts established with the glass plates of the cell using the matching fluid. The pyramids and the matching fluid

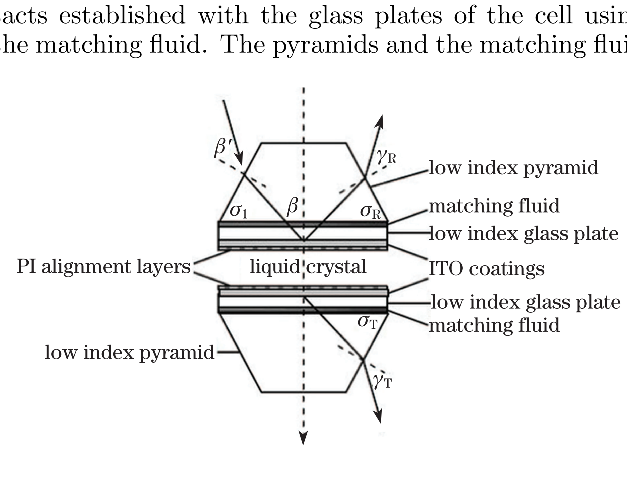

Fig. 1. Geometry of the improved fully leaky liquid crystal waveguide.

both have the same index as that of the glass plates. When a beam of light is pointed to the upper pyramid with an angle inciden β' (the external angle), the transmitted light travels in straight lines until it reaches the liquid crystal layer with an angle β (the internal angle). The relationship between these two angles can be easily obtained via the Snell law by means of the base angle of pyramid σ_{I}. Similarly, the exit angles of the reflected light and the transmitted light γ_{R} and γ_{T} can be obtained using the base angles of pyramid σ_{R} and σ_{T}, respectively.

The entire liquid crystal layer can be seen as a multi–layer optical anisotropic medium film. When the different polarized states of light (p or s) go through the liquid crystal layer, the reflected and transmitted light will produce polarization−conversion and polarization−conserving signals. These signals are controlled by the orientation of liquid crystal molecules. Thus, the distribution of the liquid crystal director must firsts be determined.

The structure of the HAN cell with thickness l and the Cartesian coordinate system are shown in Fig. 2. The z axis is along the direction normal to the substrate, and an external AC voltage U is applied into the cell along the z axis. The director's deformation is confined to the xoz plane, and the tilt angle between the director $\mathbf{n}$ and the x axis is θ, which is only dependent on the coordinate z.

The total free energy per unit area of the HAN cell is

$$F=\frac{1}{2}\int_0^l f(\theta)\theta'^2\mathrm{d}z-\frac{1}{2}\frac{U^2}{\int_0^l\frac{\mathrm{d}z}{g(\theta)}}-\frac{e_{11}+e_{33}}{2}\frac{D_z}{\Delta\varepsilon}\times\ln\left(\frac{\varepsilon_\perp+\Delta\varepsilon\sin^2\theta_l}{\varepsilon_\perp+\Delta\varepsilon\sin^2\theta_0}\right),\quad(1)$$

where $f(\theta)=k_{11}\cos^2\theta+k_{33}\sin^2\theta$, k_{11} and k_{33} are the splay and bend elastic constants. $g(\theta)=\varepsilon_0(\varepsilon_\perp+\Delta\varepsilon\sin^2\theta)$, ε_0 is the permittivity of the vacuum, $\varepsilon_\perp$ is the permittivity acrossing the long axis of the liquid crystal molecule, $\Delta\varepsilon$ is the anisotropy of the permittivity, $\theta_0=0$ and $\theta_l=90°$ are the tilt angles for the lower and the upper substrates, e_{11} and e_{33} are the splay and bend flexoelectric coefficients of the liquid crystal material, and $D_z=U/\int_0^l\frac{\mathrm{d}z}{g(\theta)}$ is the z component of the electric displacement vector. The differential equation of the director can be obtained using the variation method mentioned in Refs. [21,22]:

$$\frac{1}{2}\frac{\mathrm{d}f(\theta)}{\mathrm{d}\theta}(\theta')^2-\frac{\mathrm{d}}{\mathrm{d}z}\{f(\theta)\theta'\}-\frac{1}{2}\Delta\varepsilon D_z^2\frac{\sin2\theta}{g^2(\theta)}-\frac{e_{11}+e_{33}}{2}\frac{D_z^2}{U}\frac{\sin2\theta}{g^2(\theta)}\ln\left(\frac{\varepsilon_\perp+\Delta\varepsilon\sin^2\theta_l}{\varepsilon_\perp+\Delta\varepsilon\sin^2\theta_0}\right)=0.\quad(2)$$

Based on the differential equation, the director's deformation can be calculated using the finite difference and iterative methods[23,24]. Dividing the entire liquid crystal layer into N (N=100) sub−layers, the upper and the lower substrates correspond to the Nth and the 1st sub layer, respectively. The director of the liquid crystal will be along a certain direction and vary continuously from the lower substrate to the upper substrate. According to Ref. [25], for the same flexoelectric coefficient, the influence of the flexoelectric effect on the director in strongly anchoring HAN cell is varied, depending on different applied voltages. However, for measuring the flexoelectric coefficient through the experiment, the voltage with which the bigger variation on the director should be chosen. The applied voltage of 4 V can satisfy this requirement. Hence, this voltage is adopted in the calculation.

The distribution of the director at an external applied voltage of 4 V for different sums of the flexoelectric coefficients $e_{11}+e_{33}=\pm1.0\times10^{-11}$ C/m and $e_{11}+e_{33}=\pm2.0\times10^{-10}$ C/m is shown in Fig. 3. In calculation, the material parameters of the liquid crystal MBBA are as follows[26]: k_{11}=6.4 pN, k_{33}=8.2 pN, $\varepsilon_{//}$=4.7, $\varepsilon_\perp$=5.4, n_{e}=1.8, n_{o}=1.57. Clearly, flexoelectricity has an influence on the director in relation to the case of neglected flexoelectric effects. For the relatively small flexoelectric coefficient, the influence is weak. As the sum of the flexoelectric coefficients increases, the influence will strengthen gradually. When $e_{11}+e_{33}=\pm2.0\times10^{-10}$ C/m, a larger influence appears. These variations must induce the change of the guided mode in the improved fully leaky liquid crystal waveguide.

The measured data in the experiment denotes the relationship between the intensity of the reflected or transmitted light and the external angle β'. Thus, the reflectivity or transmittance can be determined by dividing these two beams of light by the incident light. However, comparing between the experimental and the theoretical curves requires the relationship between the reflectivity or transmittance and the internal angle β. Therefore, the transformation between β' and β needs to be ascertained using the abovementioned law. The change of the reflected and transmitted light in the liquid crystal layer

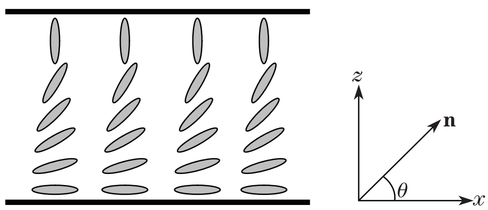

Fig. 2. Structure of the HAN cell and the Cartesian coordinate system.

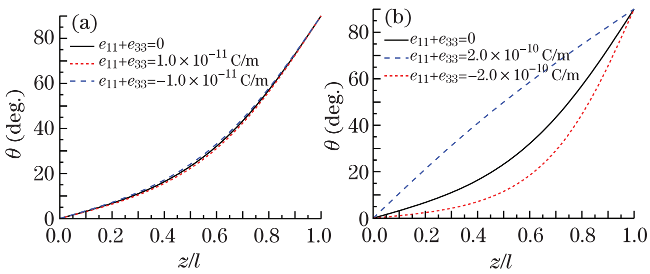

Fig. 3. Distribution of the director at an external applied voltage of 4 V for different sums of the flexoelectric coefficients (a) $e_{11}+e_{33}=\pm1.0\times10^{-11}$ C/m and (b) $e_{11}+e_{33}=\pm2.0\times10^{-10}$ C/m.

Table 1. Movement Distance Relative to the Reference Point for Different Sums of Flexoelectric Coefficients

$e_{11} + e_{33}$ ($\times 10^{-11}$ C/m)	–20	–18	–16	–14	–12	–10	–8	–6	–4
Peak Point–Reference Point	6–4	6–4	6–4	5–4	5–4	5–4	5–4	5–4	4–4
Movement Distance (deg.)	2.216	1.955	1.694	1.434	1.173	0.945	0.717	0.489	0.326
$e_{11} + e_{33}$ ($\times 10^{-11}$ C/m)	–2	–1	1	2	4	6	8	10	12
Peak Point– Reference Point	4–4	4–4	4–4	4–4	4–4	4–4	4–4	4–4	4–4
Movement Distance (deg.)	0.163	0.065	-0.065	–0.130	–0.261	–0.358	–0.456	–0.554	–0.619
$e_{11} + e_{33}$ ($\times 10^{-11}$ C/m)	14	16	18	20					
Peak Point–Reference Point	3–4	3–4	3–4	3–4					
Movement Distance (deg.)	–0.717	–0.782	–0.847	–0.880					

can be calculated using the multi−layer optical theory[27,28]. Moreover, the relationship between the reflectivity or transmittance out of the pyramid and the internal angle can be obtained from the Fresnel formula. Through numerical simulation, the fully leaky guided mode is found sensitively to the p-polarized light, especially the reflectivity $R_{\rm pp}$ and the transmittance $T_{\rm ps}$. Here, reflectivity $R_{\rm pp}$ versus the internal angle for the improved fully leaky guided mode geometry, with different sums of the flexoelectric coefficients at an external applied voltage of 4 V, is given in Fig. 4. The material parameters of liquid crystals are similar to the calculation of the distribution of the director. The thicknesses of the ITO and PI layers are 25 and 85 nm, and the permittivities of these two layers are $\varepsilon_{//}=\varepsilon_{\perp}$=3.3+i0.155 and $\varepsilon_{//}=\varepsilon_{\perp}$=1.9+i0.015, respectively. The base angles of the pyramid are equal to 60°, namely, $\sigma_{\rm I}=\sigma_{\rm R}=\sigma_{\rm T}$=60°. The wavelength of the beam of light is λ=632.8 nm.

The curve of reflectivity $R_{\rm pp}$ versus the internal angle will move a distance to the left or the right when the sign of the sum of flexoelectric coefficients is + or –, shown in Fig. 4(a). With the increase of the absolute value of the sum of flexoelectric coefficients, the distance of movement will also increase. When the absolute value is bigger, 1–2 offsets of peak value becomes relative to the neglected flexoelectric effect, as shown in Fig. 4(b). If the curve with $e_{11} + e_{33}$=0 is set to the reference curve, the fourth peak is taken as the reference point. Comparing the two other curves with the reference curve, the distance of movement of the internal angle can be obtained. For example, when $e_{11} + e_{33}$=–2.0×10^{-10} C/m, the sixth peak corresponds to the reference point, and the difference in value between them is 2.216°. The other distances of movement for different sums of flexoelectric coefficients are listed in Table 1.

According to the listed data, the relationship between the movement distance and the sum of flexoelectric coefficients can be plotted, as shown in Fig. 5. The variation of the movement distance with the value of $e_{11} + e_{33}$ is nonlinear. The influence of the negative flexoelectric coefficient on the movement distance is greater than that of the positive case. Therefore, the sum of flexoelectric coefficients can be determined provided that the movement distance is measured by the improved fully leaky guided mode technique.

In conclusion, we discuss the exploration of the sum of flexoelectric coefficients e_{11} and e_{33} of NLCs. The detailed numerical results of both the distribution of the director in the strongly anchored HAN cell and the polarization–conserving reflectivity $R_{\rm pp}$ of the improved fully leaky waveguide geometry comprising the pyramid and the HAN cell are presented. The influence of the flexoelectric effect is also analyzed in detail. The difference of the sum of flexoelectric coefficients has an effect on the curve of the $R_{\rm pp}$-internal angle, and results in different movement distances of the internal angle. By measuring the movement distance, the sum of flexoelectric coefficients e_{11} and e_{33} can be obtained.

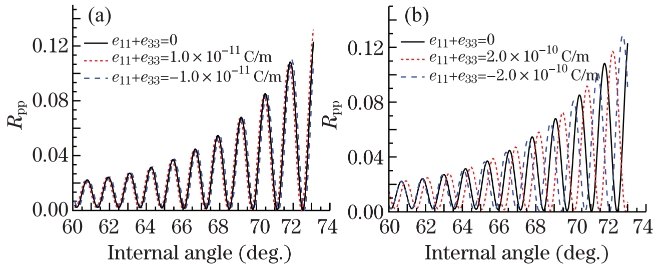

Fig. 4. Reflectivity $R_{\rm pp}$ versus the internal angle for the improved fully leaky guided mode geometry with different sums of the flexoelectric coefficients at an external applied voltage of 4 V (a) $e_{11} + e_{33}$ = ±1.0×10^{-11} C/m and (b) $e_{11} + e_{33}$ = ±2.0×10^{-10} C/m.

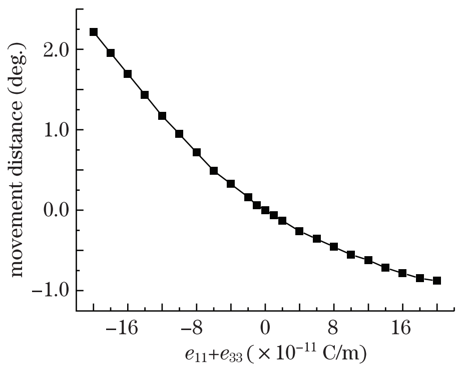

Fig. 5. Dependence of movement distance on the sum of flexoelectric coefficients $e_{11} + e_{33}$ for the external applied voltage of 4 V.

The authors would like to thank Prof. F. Z. Yang for the theoretical and experimental help. This work was supported by the Natural Science Foundation of Hebei Province (No. A2010000004), the National Natural Science Foundation of China (Nos. 60878047, 10974042, 11147103, and 60736042), the Key Subject Construction Project of Hebei Province University, and the Research Project of Hebei Education Department (No. Z2011133).

References

1. D. K. Yang and S. T. Wu, *Fundamentals of Liquid Crystal Devices* (Wiley, Chichester, 2006).
2. B. Ma, B. Yao, S. Yan, F. Peng, J. Min, M. Lei, and T. Ye, Chin. Opt. Lett. **8,** 960 (2010).
3. R. B. Meyer, Phys. Rev. Lett. **22,** 918 (1969).
4. J. S. Patel and R. B. Meyer, Phys. Rev. Lett. **58,** 1538 (1987).
5. G. Derfel and M. Buczkowska, Liq. Cryst. **34,** 113 (2007).
6. W. Ye, H. Xing, Z. Ren, Z. Zhang, Y. Sun, and G. Chen, Chin. Opt. Lett. **8,** 1171 (2010).
7. Y. Xiang, Y. K. Liu, X. S. Xie, J. M. Li, J. H. Wang, and Z. G. Cai, Appl. Phys. Lett. **97,** 203507 (2010).
8. L. M. Blinov and V. G. Chigrinov, *Electrooptic Effects in Liquid Crystals Materials* (Springer-Verlag, New York, 1994).
9. J. Harden, B. Mbanga, N. Eber, K. F. -Csorba, S. Sprunt, J. T. Gleeson, and A. Jli, Phys. Rev. Lett. **97,** 157802 (2006).
10. J. Harden, M. Chambers, R. Verduzco, P. Luchette, J. T. Gleeson, S. Sprunt, and A. Jákli, Appl. Phys. Lett. **96,** 102907 (2010).
11. T. Takahashi, S. Hashidate, H. Nishijou, M. Usui, M. Kimura, and T. Akahane, Jpn. J. Appl. Phys. **37,** 1865 (1998).
12. C. L. Trabi, A. A. T. Smith, and C. V. Brown, Mol. Cryst. Liq. Cryst. **509,** 378 (2009).
13. C. Kischka, L. A. P.-Jones, S. J. Elston, and E. P. Raynes, Mol. Cryst. Liq. Cryst. **480,** 103 (2008).
14. C. Kischka, S. J. Elston, and E. P. Raynes, Mol. Cryst. Liq. Cryst. **494,** 93 (2008).
15. A. Mazzulla, F. Ciuchi, and J. R. Sambles, Phys. Rev. E **64,** 021708 (2001).
16. H. M. Sykulska, L. A. P.-Jones, and S. J. Elston, Mol. Cryst. Liq. Cryst. **436,** 267 (2005).
17. C. L. Trabi, A. A. T. Smith, C. V. Brown, and N. J. Mottram, Appl. Phys. Lett. **92,** 223509 (2008).
18. F. Z. Yang and J. R. Samble, J. Opt. Soc. Am. B **10,** 858 (1993).
19. F. Z. Yang and J. R. Samble, in *Nanotechnology and NICE Devices* (Taloy and Francis, Oxford, 2003).
20. F. Z. Yang and J. R. Samble, J. Opt. Soc. Am. B **16,** 488 (1998).
21. Y. Z. Xie, *Physics of Liquid Crystal* (in Chinese) (Science press, Beijing, 1998).
22. W. J. Ye, H. Y. Xing, G. C. Yang, and M. Y. Yuan, Chin. Phys. B **18,** 238 (2009).
23. Q. Wang and S. L. He, Acta Phys. Sin. (in Chinese) **50,** 926 (2001).
24. W. J. Ye, H. Y. Xing, G. C. Yang, Z. D. Zhang, Y. B. Sun, and G. Y. Chen, Commun. Theor. Phys. **55,** 340 (2011).
25. W. J. Ye, H. Y. Xing, and G. C. Yang, Chin. J. Comput. Phys. (in Chinese) **24,** 337 (2007).
26. N. T. Kirkman, T. Stirner, and W. E. Hagston, Liq. Cryst. **30,** 1115 (2003).
27. D. W. Berreman, J. Opt. Soc. Am. **62,** 502 (1972).
28. D. W. Berreman, J. Opt. Soc. Am. **63,** 1374 (1973).